

Probabilistic Capacity Models for Corroding Posttensioning Strands Calibrated Using Laboratory Results

Paolo Gardoni, M.ASCE¹; Radhakrishna G. Pillai²; Mary Beth D. Hueste, P.E., M.ASCE³; Kenneth Reinschmidt, P.E., M.ASCE⁴; and David Trejo, P.E., M.ASCE⁵

Abstract: The presence of air voids, moisture, and chlorides inside tendons or ducts was cited as a reason for the early age strand corrosion and failure in the Mid-bay, Sunshine Skyway, and Niles Channel posttensioned (PT) bridges in Florida, United States. Although rare, these incidents call for frequent inspection and structural reliability assessment of PT bridges exposed to moisture and chlorides. This paper develops and presents probabilistic strand capacity models that are needed to assess the structural reliability of such PT bridges and recommends a time frequency of inspection. A total of 384 strand test specimens were exposed to various void, moisture, and chloride concentration conditions for 12 and 21 months; the remaining tension capacities were then determined. Using this experimental data and a Bayesian approach, six probabilistic capacity models were developed based on the void type. The mean absolute percentage errors of these models are less than 4%, indicating that reasonably accurate prediction of the strand capacity is possible, when void, aggressive moisture, and chloride conditions are present.

DOI: 10.1061/(ASCE)EM.1943-7889.0000021

CE Database subject headings: Chlorides; Corrosion; Tension; Voids; Ducts; Bridges; Florida; Probability; Capacity.

Introduction

The construction of long span, posttensioned (PT), segmental concrete bridges began in the United States in the 1960s. Fig. 1 shows a typical interior view of box girders in PT segmental concrete bridges. Until recently, the PT structures in the United States were thought to be highly durable and resistant to corrosion. In most PT bridges, this is actually the case. However, NCHRP (1998), ASBI (2000), and FDOT (2001a,b) reported the presence of air voids (voids herein) and corroded strands in the grouted tendons on PT bridges. Fig. 2 shows typical no-void and void conditions inside the tendons. According to Schupack (2004), the evaporation of bleedwater and the poor grouting and construction practices are possible reasons for the unwanted void formation inside the tendons. The presence of moisture and chlorides inside the voids caused early age corrosion-induced failures of strands in the Mid-Bay, Sunshine Skyway, and Niles Channel

Bridges in Florida at 8, 13, and 16 years, respectively, after construction (NCHRP 1998; ASBI 2000; FDOT 2001a,b). In addition, Woodward et al. (2001) inspected 281 PT bridges in the United Kingdom and reported that the presence of water, sometimes with chloride contaminated grout, was found in 13% of the tendons. Voids were also present in most of these tendons. The presence of voids and water can cause corrosion, resulting in the reduction in the tensile strength capacity (capacity herein) of the strands. Poston et al. (2003) reported that a 25% reduction in strand capacity can result in 50% or more reduction in live load carrying capacity of the bridge. These studies and field observations indicate the dire need to develop time-variant structural reliability models for these bridge structures.

In general, nominal capacity (\hat{c}) of strands can be used for structural reliability assessment when strands are in pristine conditions with no reduction in capacity. In this paper, \hat{c} is defined as being equal to the minimum ultimate tensile strength (MUTS) of strand. According to PTI (1998), MUTS of a strand is defined as the force equal to the nominal cross-sectional area of strand times their nominal ultimate tensile stress. Therefore, MUTS or \hat{c} of a 270-ksi (1,860 N/mm²) grade 0.6-in. (15.24 mm) diameter seven-wire strand meeting the ASTM A416 specification is 58.6 kips (261 kN). However, for PT bridges experiencing aggressive corrosive conditions, the structural reliability should be assessed using probabilistic strand capacity models that account for the loss in capacity over time instead of \hat{c} . Historically, engineers have developed deterministic empirical models based on research findings. Following this practice, six usable probabilistic strand capacity models are developed based on a comprehensive experimental program and are presented in this paper.

This paper is organized as follows. First, a brief overview of the experimental program and design is presented. Then, a statistical modeling of the strand capacity is presented with details on the diagnostic studies and identification of important and unimportant test variables. Probabilistic capacity model formulation

¹Associate Professor, Zachry Dept. of Civil Engineering, Texas A&M Univ., 3136 TAMU, College Station, TX 77843-3136 (corresponding author). E-mail: pgardoni@civil.tamu.edu

²Graduate Student, Zachry Dept. of Civil Engineering, Texas A&M Univ., 3136 TAMU, College Station, TX 77843-3136.

³E.B. Snead II Associate Professor, Zachry Dept. of Civil Engineering, Texas A&M Univ., 3136 TAMU, College Station, TX 77843-3136.

⁴J. L. Frank/Marathon Ashland Petroleum LLC Chair in Engineering, Project Management Professor, Zachry Dept. of Civil Engineering, Texas A&M Univ., 3136 TAMU, College Station, TX 77843-3136.

⁵Zachry Career Development Professor I, Zachry Dept. of Civil Engineering, Texas A&M Univ., 3136 TAMU, College Station, TX 77843-3136.

Note. This manuscript was submitted on March 1, 2008; approved on January 14, 2009; published online on March 6, 2009. Discussion period open until February 1, 2010; separate discussions must be submitted for individual papers. This paper is part of the *Journal of Engineering Mechanics*, Vol. 135, No. 9, September 1, 2009. ©ASCE, ISSN 0733-9399/2009/9-906-916/\$25.00.



Fig. 1. Typical interior view of box girders in PT bridges (six external tendons are visible)

and assessment procedures are presented prior to the results and discussions. Practical applications of the developed models are discussed before the conclusions.

Overview of Experimental Program and Design

A 12- and 21-month long strand corrosion (SC) test program was conducted to generate the data necessary to formulate, develop, and assess the probabilistic capacity models. This study used 0.6-in. (15-mm) diameter low relaxation seven-wire strands that meet the requirements of “Standard specification for steel strand, uncoated seven-wire for prestressed concrete” (ASTM 2006). A total of 384 strand test specimens [each 41-in. (1,040 mm) long] with grout class (GC) and void type (VT) as *qualitative variables* (i.e., variables with different factors) and moisture content (MC), chloride concentration ($\%Cl^-$), and wet-dry exposure time (t_{WD}) as *quantitative variables* (i.e., variables with different levels) were prepared. Each test specimen was then concurrently exposed to a particular factor and/or level of each qualitative and quantitative variable. The experimental design of the variables used in this analytical study is provided in Table 1. Then, probabilistic capacity models were developed using the experimental data from unstressed SC samples exposed for 12 and/or 21 months. A brief description of test variables used in this analytical study is provided next.

In the United States, the Post-Tensioning Institute (PTI) classifies grout materials into four types or classes based on material specifications and field requirements (PTI 2003). In general, Class A and Class C grouts have been used in most PT bridges in the United States. Hence, in this study, Class A grout with 0.44 water-cement ratio (w/c) and Class C grout with 0.27 w/c were used.

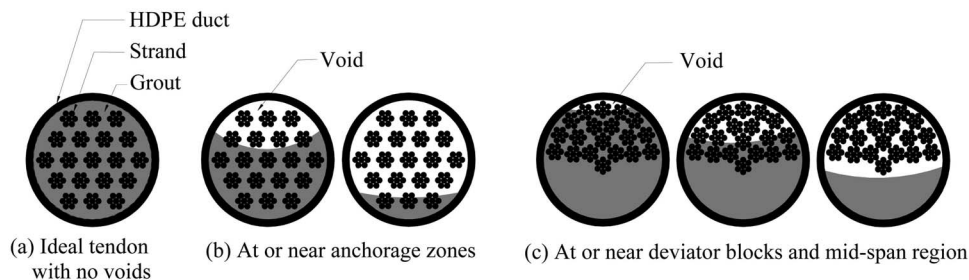


Fig. 2. Cross sections showing typical no-void and void conditions inside a PT duct (adapted from Trejo et al. 2009a)

Table 1. Experimental Design Showing the Number of Test Specimens with Each Variable Combination

Grout type	Exposure time t (months)	$\%Cl^-$	VT				
			NV	BV	IV	OV	PV
Class A	12	0.006	5	5	5	5	5
		0.018	5	5	5	5	5
		0.18	5	—	5	5	5
		1.8	5	5	5	3	3
	21	0.006	5	5	5	5	5
		0.018	5	5	5	5	5
		0.18	5	—	5	5	5
		1.8	5	5	5	4	4
		1.8	5	5	5	5	5
Class C	12	0.006	5	5	5	5	5
		0.018	5	5	5	5	5
		0.18	5	—	5	5	5
		1.8	5	5	5	5	5
	21	0.006	5	5	5	5	5
		0.018	5	5	5	5	5
		0.18	5	—	5	5	5
		1.8	5	5	5	5	5
		1.8	5	5	5	5	5

Note: Capacities of ten pristine strands were also tested and assigned $\%Cl^- = 0.0001$ and $t = 0$.

The qualitative variable, VT, was used to discriminate between five possible field void conditions (see Fig. 3) defined as follows:

- No void (NV)—The condition when tendons are fully grouted.
- Parallel void (PV). The longitudinal axis of the partially embedded strand is parallel to the grout surface. This void condition is typically found in the midspan region of the PT bridges with a horizontal tendon profile.
- Orthogonal void (OV)—The longitudinal axis of the partially embedded strand is orthogonal to the grout surface. This void condition is typically found in PT columns or piers or other elements with a vertical profile. Nevertheless, depending on the flow characteristics of fresh grout, the OV type may also be found in PT ducts with horizontal or inclined profiles.
- Inclined void (IV)—The longitudinal axis of the partially embedded strand is at 45° to the grout surface. This void condition is typically found near anchorage zones of the PT bridges with tendons in inclined position.
- Bleedwater void (BV)—The void condition formed due to the evaporation of bleedwater. Note that the thin grout layer on strand surface near void location (shown as “GS” in Fig. 3) is the only difference between the BV and IV samples.

These VTs are intended to represent typical geometries of grout-air-strand (GAS) interfaces that are found in PT bridges and

Notes: E - Epoxy; G - Grout; M - Mold; P - Ponding solution; R - Reservoir; S - Strand; GS - Grout layered strand

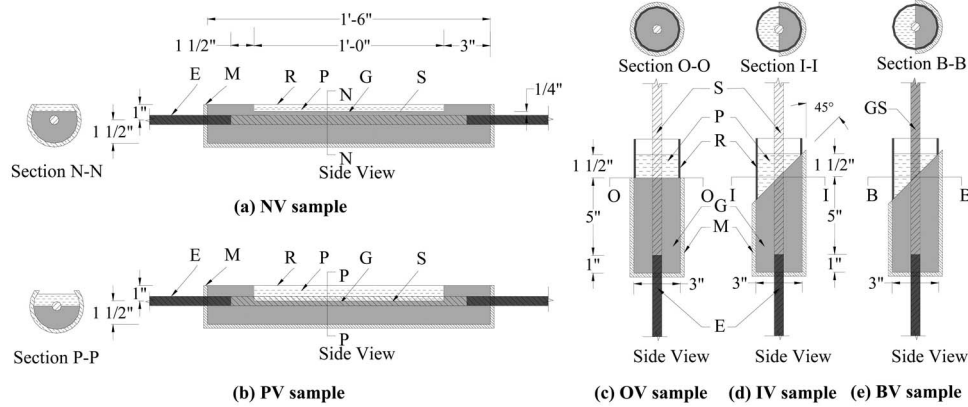


Fig. 3. Schematics of NV, PV, OV, IV, and BV samples [Note: 1" = 25.4 mm] (adapted from Trejo et al. 2009a, 200%)

can cause varying degrees of localized SC. Also, a general void condition consisting of an assumed equal distribution of BV, IV, OV, and PV is defined and referred to as all-void (AV) condition. This condition should be used when it is known that voids exist and there is no knowledge about the GAS geometry. These GAS geometries can result in varying degrees of localized SC. For this reason, a probabilistic capacity model is constructed for each VT. Moisture or water at the metal surface is an essential component for electrochemical corrosion process of steel embedded in cementitious materials (ACI 2003). It should be noted that all the test specimens (except pristine strands) underwent cyclic wet-dry (WD) exposure. Because only one MC level (i.e., 100%) is used in this analytical study, it is not explicitly shown in the experimental design in Table 1. The corrosion processes worsen when the (%Cl⁻) at the strand surfaces increases and reaches a threshold level. However, the chloride threshold level was found to be unnecessary for the topic of this paper (i.e., capacity loss of strands). As shown in Table 1, the SC specimens were exposed at 0.0001, 0.006, 0.018, 0.18, and 1.8%Cl⁻. A concentration of 0.0001%Cl⁻ was assigned to pristine strand samples. The probabilistic capacity models, presented later, are formulated using the natural logarithm of %Cl⁻. Because the ln[zero] is indeterminate, the small value 0.0001%, that is close to zero, is chosen to avoid mathematical challenges. It is well known that the corrosion of steel embedded in cementitious materials is a time-dependent process. In this test program, two levels of the quantitative variable, t_{WD} , are considered (i.e., 12 and 21 months).

Prior to presenting the statistical modeling, a brief description on the type of corrosion observed is also provided next. All the strands experienced maximum localized corrosion at or near the GAS interfaces. The strands exposed to 0.006%Cl⁻ solution exhibited uniform corrosion and that exposed to 0.018, 0.18, and 1.8%Cl⁻ solutions exhibited pitting corrosion. Further details on this are given in Trejo et al. (2009a,b) and Pillai (2009).

Statistical Modeling

As a first step in the modeling process, diagnostic plots are developed to study the effect of each qualitative and quantitative variable on the strand capacity. Then, based on corrosion and mathematical principles, the test variables are classified as unimportant and important variables. Probabilistic capacity models are then developed using the important variables and are assessed

using the experimental data. The results from the diagnostic study on the effects of the important and unimportant variables on strand capacity are provided next.

Unimportant Variables

The corrosivity of the cementitious grout depends on the qualitative variable, GC, representing the combined effect of the chemical composition and w/c of grout. The corrosion mechanisms for a strand system containing a void and a system containing no void (NV) are different and the presence of the void would be expected to have a more significant effect on the corrosion rate than grout material characteristics such as chemical composition and w/c. This study evaluated the potential influence of GC and VT and not that of w/c. The diagnostic study indicates that GC is not a critical variable directly influencing the SC and capacity. In other words, both Class A and Class C grouts caused similar reduction in capacity, provided all other variables remained the same. Hence, GC is not considered in the formulation of the probabilistic models. However, it should be noted that the probability of formation of voids inside the ducts during construction is likely dependent on the GC used.

Important Variables

The diagnostic plots shown in Figs. 4 and 5 indicate that VT, %Cl⁻, t_{WD} , and the interaction between %Cl⁻ and t_{WD} are important variables that affect the strand capacity. Note that these basic important variables are appropriately included in the probabilistic model formulations provided in this paper.

Void Type

Figs. 4(a and b) show the effect of VT on the remaining strand capacity at 12 and 21 months of WD exposure cycles, respectively. Each data marker represents the residual capacity of a tested strand specimen. Each column of data markers corresponds to a specific VT at either 12 or 21 months of exposure and the thick horizontal lines indicate the mean capacities. In Figs. 4(a and b), the dot plot on the extreme left [indicated by open square markers (□)] shows the observed capacities of the pristine strands; the mean observed capacity is equal to 60.5 kips (≈268.5 kN). In general, samples with NV and PV conditions experienced less reduction in capacity and less scatter when compared to samples with BV, IV, and OV conditions, considering

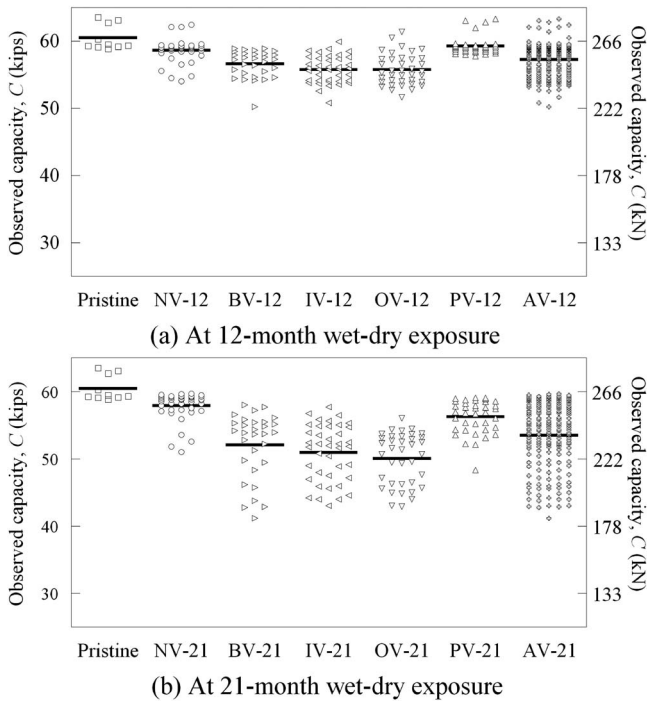


Fig. 4. Effect of VT on strand capacity

both the 12- and the 21-month data. Figs. 4(a and b) also show that there is a slight reduction in capacity with the NV condition, indicating that the presence of voids is not absolutely essential for capacity reduction. In summary, VT significantly influences the strand capacity. Hence, a total of six probabilistic models (i.e., one for each VT defined earlier) are developed.

Chloride Concentration

The scatter plots in Fig. 5(a) indicate a linear trend between the mean observed capacity and the natural logarithm of $\%Cl^-$. The vertical text next to the data points indicates the actual $\%Cl^-$ values corresponding to the $\ln[\%Cl^-]$ values on the abscissa. Because of the high coefficients of determination, R^2 , ranging from 0.74–0.98, a linear function of $\ln[\%Cl^-]$ is appropriate to capture the dependence of the capacity on $\%Cl^-$.

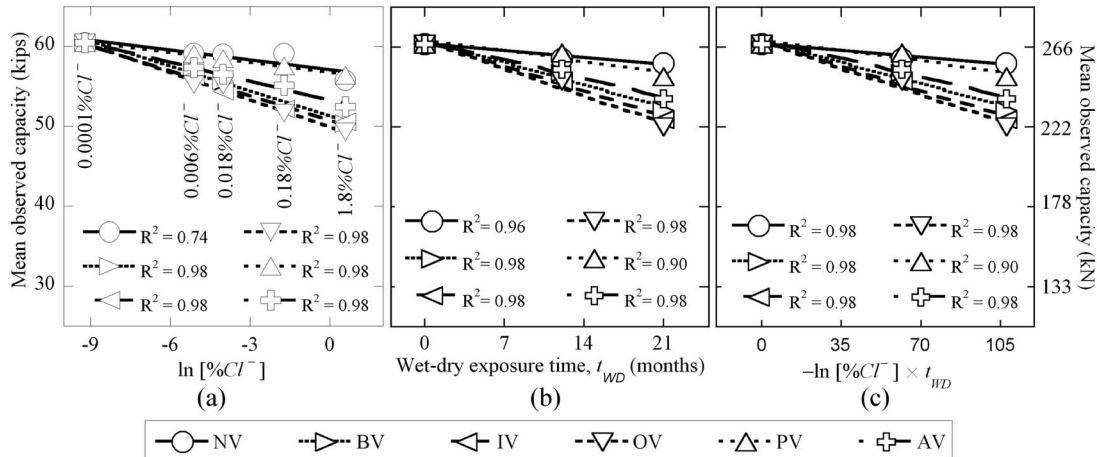


Fig. 5. Effect of important predictor variables on capacity of strands exposed to various VTs

Wet-Dry Exposure Time

As is the case of $\ln[\%Cl^-]$, Fig. 5(b) indicates that the relationship between the mean observed capacity and t_{WD} is approximately linear. The linear fits in Fig. 5(b) exhibit high R^2 values ranging from 0.90–0.98. Hence, a linear function of t_{WD} is used to construct the probabilistic models presented in this paper.

Two-Way Interaction between $\%Cl^-$ and t_{WD}

Fig. 5(c) shows the diagnostic plot between the mean observed capacity and the two-way interaction term $(-\ln[\%Cl^-] \times t_{WD})$. The negative sign is included here merely to improve the presentation and readability of the similar linear trends in all three plots in Fig. 5. In the statistical modeling, which will be presented later, this negative sign is not included. The presence of the interaction term in the formulation of the probabilistic capacity model can be justified from an electrochemical corrosion point because either a high t_{WD} value alone with zero $\%Cl^-$ (for instance, no chlorides for 100 years) or a high $\%Cl^-$ value alone with zero t_{WD} (for instance, seawater for 1 day) do not normally lead to significant corrosion and reduction in capacity. From a statistical standpoint, the interaction term helps satisfy the homoskedasticity and normality assumptions that are needed to properly assess the model by statistical analysis. The homoskedasticity assumption means that the variance of the model error is approximately constant and independent of the predictor variables. The normality assumption means that the model error follows a normal distribution. The scope of the experimental data used for developing the probabilistic models is only up to 21 months (i.e., 1.75 years). Therefore, the use of the developed models for $t_{WD} > 1.75$ years needs to be reasonably justified or a correlation with actual conditions needs to be determined. The authors are in the process of inspecting PT bridges to determine the validity of these models.

In electrochemical reactions, the rate of weight loss of steel can be expressed as follows:

$$W = i_{avg} \cdot D \cdot A_{exp} \cdot t_{exp} \quad (1)$$

where W =weight loss in kilograms (or pounds); i_{avg} =average corrosion rate in meters per second (or inches per second); D =density of steel in kg/m^3 ($lb/in.^3$); A_{exp} =area of exposed curved surface in m^2 ($in.^2$); and t_{exp} =exposure period in seconds. Although i_{avg} may not be constant, it is common in the literature to assume that this value is constant. For example, Akgul and

Frangopol (2004) assumed i_{avg} for prestressing steel in chloride-contaminated prestressed concrete can be assumed to be 2.25 mils/year (0.0572 mm/year). Also, the figures in Melchers (2003) suggest that a linear corrosion loss assumption is reasonable for long term immersion corrosion of alloy steels. In addition, A_{exp} of a cylindrical PT wire is equal to $2\pi rl$ (r =radius, l =length) and the rate of change of r can be assumed equal to its i_{avg} . Based on these assumptions and using Eq. (1), it can be assumed that W varies linearly as a function of t_{exp} . Because the cross-sectional area, A , is directly related to W , the rate of loss of A is assumed to be linear with time (i.e., dA/dt =constant). Nevertheless, because the capacity of a strand is proportional to A , the rate of loss of capacity is linear with time. This indicates that the use of linear functions of t_{WD} , for a given %Cl⁻ (i.e., $\propto t_{WD}$ and $\ln[\%Cl^-] \times t_{WD}$) in the probabilistic capacity models is reasonable. The probabilistic model assessed using the available data can also be used to approximately forecast the capacity when t_{WD} is greater than 1.75 years.

Formulation of Probabilistic Capacity Models

Gardoni et al. (2002) formulated probabilistic capacity models for reinforced concrete bridge systems. These models can be used for modeling strand capacity as follows:

$$R_C(\mathbf{x}, \Theta) = \gamma(\mathbf{x}, \Theta) + \sigma \varepsilon \quad (2)$$

where $R_C(\mathbf{x}, \Theta)$ =ratio between the actual strand capacity $C(\mathbf{x}, \Theta)$ and the nominal strand capacity \hat{c} ; $\gamma(\mathbf{x}, \Theta)$ =capacity correction function; \mathbf{x} =vectors of the basic qualitative and quantitative variables; $\Theta=(\theta, \sigma)$ =vectors of unknown parameters, where $\theta=(\theta_1, \dots, \theta_k)$ is a $k \times 1$ vector of the model parameter and k =number of regressors; and $\sigma \varepsilon$ =model error, where σ represents the standard deviation (SD) of the model error and ε =random variable with zero mean and unit SD. Note that for a given \mathbf{x} , θ , and σ , the model variance $\text{var}[R_C(\mathbf{x}, \Theta)]$ is equal to σ^2 . Therefore, σ^2 (or σ) can be used as a measure of the model accuracy.

A dimensionless model has two benefits over one with specific physical dimensions. First, in the case of a dimensionless model, the model parameters are also dimensionless so that the model can be used with any unit. Second, a dimensionless model is applicable when the standardized variables fall within range of the standardized variables in the database. This typically expands the range of applicability of the model. The term $R_C(\mathbf{x}, \Theta)$ is dimensionless because it is a ratio between $C(\mathbf{x}, \Theta)$ and \hat{c} that are measured in identical units. In addition, $\gamma(\mathbf{x}, \Theta)$ is developed using the standardized functions of the basic variables. These standardized functions are shown in Eqs. (3) and (4)

$$\gamma_{Cl^-} = \left(\frac{\ln[\%Cl^-]}{\ln[\%Cl^-_{seawater}]} \right) \quad (3)$$

$$\gamma_t = \left(\frac{t_{WD}}{t_{curing}} \right) \quad (4)$$

The units of numerators and denominators in Eqs. (3) and (4) are identical. The models developed in this paper are calibrated using $\%Cl^-_{seawater}$ and t_{curing} equal to 2.12%Cl⁻ and 0.93 months, respectively. The proposed model form is dimensionless because of the use of standardized predictor variables and $R_C(\mathbf{x}, \Theta)$. As a result, the parameters θ_j are also dimensionless. Appropriate conversion factors must be employed if the user changes the units of numerators in Eqs. (3) and (4) from %Cl⁻ and months, respec-

tively. The correction function, $\gamma(\mathbf{x}, \Theta)$, captures two reasons why the actual capacity might be different from the nominal one: (1) the actual capacity of a pristine strand is typically greater than the nominal capacity because of potential *liability concerns* with the producing company and (2) corrosion might lead to a reduction in the capacity.

Scatter plots of the residuals and observed capacities against predicted capacities verify that the homoskedasticity and the normality assumptions are satisfied for this model formulation. These are not shown here due to space limitations. The next section develops capacity models based on the observations made on the diagnostic plots and the model formulation provided in Eq. (2).

Development of Probabilistic Capacity Models

Individual probabilistic models are developed for each VT (i.e., Models NV, BV, IV, OV, and PV) using the predictors γ_{Cl^-} , γ_t , and $\gamma_{Cl^-}\gamma_t$. Because of the length of actual tendons (i.e., several miles) in PT bridges and other technical difficulties associated with the bridge inspection procedures, it might be difficult to identify and quantify the actual VTs existing in a PT segment. Hence, though VT is a critical variable, a general capacity model (i.e., Model AV) is developed using all the experimental data (except data from NV samples) with no distinction on the VT. Therefore, *Model AV* is based on the data from all the 304 test specimens shown in Table 1 and can be used when the types of voids existing inside the PT ducts are unknown and all are considered equally likely.

All six probabilistic models can be generally expressed as follows:

$$R_C(\mathbf{x}, \Theta) = \theta_1 + \theta_2(\gamma_{Cl^-}) + \theta_3(\gamma_t) + \theta_4(\gamma_{Cl^-}\gamma_t) + \sigma \varepsilon \quad (5)$$

where the terms are defined in Eqs. (2)–(4).

Methodology for the Assessment of Probabilistic Capacity Models

The probabilistic model in Eq. (3) is linear in its parameters, no prior information is available about the distribution of Θ and no upper or lower bound data are used. The Bayesian closed-form solution procedures provided in Box and Tiao (1992) can be used to assess such probabilistic models.

Posterior Statistics of Model Parameters

The linear probabilistic models can be written in the following general form:

$$R_C = G\Theta + \sigma \varepsilon \quad (6)$$

where $R_C = n \times 1$ vector of capacity observations (R_{C1}, \dots, R_{Cn}); n =number of observations or sample size; $G = n \times k$ matrix of known regressors; k =number of regression parameters (in this study, $k=4$); and $\varepsilon = n \times 1$ vector of normal random variables [i.e., $\varepsilon \sim N(0, 1)$]. The remaining quantities are defined in Eq. (2). Box and Tiao (1992) provides expressions for posterior statistics of Θ as follows:

$$p(\Theta|R_C) \propto p(\Theta)p(s^2|\sigma^2)p(\hat{\theta}|\theta, \sigma^2) \quad (7)$$

where $\hat{\theta} = (G^T G)^{-1} G^T R_C$; $s^2 = (1/v)(R_C - \hat{R}_C)^T (R_C - \hat{R}_C)$; $v = n - k$; and $\hat{R}_C = G\hat{\theta}$.

The marginal posterior distribution of θ follows a multivariate student t -distribution, $t_k[\hat{\theta}, s^2(G^T G)^{-1}, v]$, where $\hat{\theta}$ is both the mode and the mean of θ and the covariance matrix is

$vs^2(G^T G)^{-1}/(v-2)$. The marginal posterior distribution of σ^2 is $vs^2\chi_v^{-2}$, where χ_v^{-2} is the inverted chi-square distribution with v degrees of freedom, mean $vs^2/(v-2)$, and variance $2v^2s^4/[(v-2)^2(v-4)]$.

Mean Absolute Percentage Error

As noted earlier, σ can be used to measure the model accuracy. In addition to this, the mean absolute percentage error (MAPE) can be used to provide a more intuitive measure of the model accuracy. The MAPE is the average error in the model expressed as a percent of the measured value and can be mathematically expressed as follows:

$$\text{MAPE} = \frac{1}{n} \left[\sum_{i=1}^n \left\{ \frac{|E[C(\mathbf{x}_i, \boldsymbol{\theta})] - C_i|}{C_i} \right\} \right] \times 100 \quad (8)$$

where C_i = observed capacity and $E[C(\mathbf{x}_i, \boldsymbol{\theta})] = \hat{c}\gamma(\mathbf{x}_i, \hat{\boldsymbol{\theta}})$ = mean predicted capacity.

Selection of the Most Parsimonious Parameter Set

Although the diagnostic plots can assist in identifying the unimportant and important predictor variables, their selection needs to be justified for being the most parsimonious parameter set (i.e., as few parameters θ_i as possible). In other words, from a statistical standpoint, to avoid the loss of precision on the estimates of the parameters and on the overall model (due to the inclusion of statistically redundant variables) and overfitting the data, a model should have parsimonious parameterization. To attain such a model, a stepwise variable deletion process (Gardoni et al. 2002) can be carried out on the full model under consideration [in this case, Eq. (5)]. The coefficient of variation (CoV) of the parameter estimates in the full and reduced models (i.e., models with fewer variables than full model) and the MAPE and σ^2 of the full and reduced models can be compared to determine the most parsimonious model. In addition, engineering judgment could, and should, play a role in the final model selection.

Results and Discussions

The formulation presented in the previous section is used here to assess the six probabilistic capacity models (Models NV, BV, IV, OV, PV, and AV) based on the experimental data. Prior to discussing the specific characteristics of each of these models, a brief discussion on the selection of the most parsimonious parameter set is presented.

Most Parsimonious Parameter Set

To identify the most parsimonious model form, a stepwise deletion process was carried out with the model in Eq. (5) as the full model. In general, for Models NV, BV, IV, OV, PV, and AV, the CoV of θ_2 , which is the coefficient of γ_{Cl^-} , was found to be larger in absolute magnitude when compared to that of the other parameters in the full model form [Eq. (5)]. This indicates that the confidence level on the estimated value of θ_2 is smaller than that of the other parameters in Eq. (5). However, removing γ_{Cl^-} from Eq. (5) led to a slightly larger MAPE and significantly larger σ^2 , indicating a reduction in overall model quality. Hence, considering the term γ_{Cl^-} as an important predictor variable is justified and Eq. (5) is the most parsimonious model, considering practical engineering and the available data set.

Assessment of Probabilistic Capacity Models

Table 2 summarizes the MAPE and posterior statistics of the model parameters for Models NV, BV, IV, OV, PV, and AV. The model parameters θ_1 , θ_2 , θ_3 , and θ_4 correspond to the intercept γ_{Cl^-} , γ_t , and $\gamma_{\text{Cl}^-}\gamma_t$ terms, respectively. Figs. 6(a–f) show the comparison between the observed and the predicted capacities for the six capacity models. For a perfect prediction model, the predicted and observed capacities should line up along the 1:1 solid lines. However, due to measurement errors and model errors due to missing variables in Eq. (2) or an inaccurate model form, there is a scatter around the 1:1 line. In particular, different capacities are observed for test samples that have identical combinations of test variables. The two dashed lines delimit the region within one SD from the 1:1 line. The rhombic (\diamond) and triangular (\triangle) data markers indicate the 12- and 21-month data, respectively. Fig. 6 shows that the selected models have no systematic bias or residual trend and that the homoskedasticity and normality assumptions are approximately satisfied. Figs. 7(a–d) show the extrapolated capacities for a period of 6 years of direct attack of moisture and chlorides. The vertical dashed arrows indicate the estimated time required to reduce the strand capacity to the yield capacity (indicated by the lower horizontal dashed lines). It should be noted that the WD exposure cycles in this test program are likely more aggressive than most field conditions. The correlation between field performance and laboratory data is needed. However, such studies are not presented in this paper.

Model NV

The Model NV can be used for PT systems with completely filled or grouted tendons. The mean values of the model parameters suggest that a unit change in t_{WD} has a larger detrimental effect on capacity than a unit change in $\% \text{Cl}^-$ and/or $\% \text{Cl}^- \times t_{\text{WD}}$. Although the parameter θ_2 has a large SD, θ_1 , θ_3 , and θ_4 have small SDs, indicating signs of good confidence in their estimated values. Fig. 6(a) and the small MAPE (i.e., 1.9%) for this model indicate good accuracy of the overall model.

Model BV

The BV is possibly the most prevalent VT found in PT bridges (Schupack 2004). The Model BV indicates that when BV conditions exist, the capacity is more sensitive to t_{WD} than to $\% \text{Cl}^-$ and $\% \text{Cl}^- \times t_{\text{WD}}$. Table 2 shows that the posterior means have reasonably small SDs, showing signs of good confidence in the estimated mean values. Fig. 6(b) shows that the BV samples have a larger variability in the observed capacities resulting in a slightly wider $\pm\sigma$ band than that of Model NV. The variability in the data also resulted in a small σ^2 and a 2.4% MAPE, which is higher than that of the Model NV. However, 2.4% MAPE is reasonably good for practical bridge assessment and the model can be used when it is known that BV conditions exist.

It should be noted that there exist practical difficulties in interpreting the numerical values of the parameters in Model NV, especially in the cases of high positive correlation between θ_1 and θ_2 , θ_3 and θ_4 , and high negative correlations between θ_1 and θ_3 , θ_1 and θ_4 , θ_2 and θ_3 , and θ_2 and θ_4 . However, *when predictor variables are random variables, the multiple regression coefficients should not be simply interpreted as a relationship between the response and corresponding predictor variables* (Ryan 2007). Hence, the obtained regression coefficients are justified and, although similar high positive or negative correlations are found with remaining models, they will not be discussed herein.

Table 2. MAPE and Posterior Statistics of All the Six Probabilistic Models

Model name	MAPE (%)	Parameters	Mean	SD	Correlation coefficients among θ_i		
					θ_1	θ_2	θ_3
Model NV	1.9	θ_1	1.0111	0.0150	1		
		θ_2	-0.0017	0.0015	0.89	1	
		θ_3	-0.0023	0.0008	-0.95	-0.85	1
		θ_4	-0.0003	0.0001	-0.73	-0.81	0.83
		σ^2	0.0007	0.0001			
Model BV	2.4	θ_1	1.0948	0.0211	1		
		θ_2	0.0053	0.0020	0.92	1	
		θ_3	-0.0127	0.0012	-0.96	-0.88	1
		θ_4	-0.0012	0.0001	-0.77	-0.84	0.86
		σ^2	0.0010	0.0002			
Model IV	3.1	θ_1	1.0918	0.0202	1		
		θ_2	0.0054	0.0020	0.89	1	
		θ_3	-0.0128	0.0011	-0.95	-0.85	1
		θ_4	-0.0011	0.0001	-0.73	-0.81	0.83
		σ^2	0.0013	0.0002			
Model OV	2.8	θ_1	1.0975	0.0191	1		
		θ_2	0.0054	0.0019	0.90	1	
		θ_3	-0.0137	0.0010	-0.95	-0.86	1
		θ_4	-0.0011	0.0001	-0.72	-0.81	0.83
		σ^2	0.0010	0.0002			
Model PV	1.6	θ_1	1.1078	0.0143	1		
		θ_2	0.0065	0.0014	0.90	1	
		θ_3	-0.0083	0.0008	-0.95	-0.86	1
		θ_4	-0.0008	0.0001	-0.73	-0.81	0.83
		σ^2	0.0006	0.0001			
Model AV	4.0	θ_1	1.1001	0.0142	1		
		θ_2	0.0065	0.0018	0.81	1	
		θ_3	-0.0120	0.0008	-0.96	-0.77	1
		θ_4	-0.0011	0.0001	-0.71	-0.88	0.78
		σ^2	0.0021	0.0002			

Model IV

In general, the Model IV exhibits characteristics similar to Model BV and indicates that the capacity is, in general, more sensitive to t_{WD} than to $\%Cl^-$ and $\%Cl^- \times t_{WD}$. Table 2 shows that the posterior means have reasonably small SDs indicating high confidence levels. The scatter plot in Fig. 6(c) shows that most predicted values lie along the 1:1 line and within the $\pm\sigma$ band. The small σ^2 and MAPE (i.e., 3.1%) indicate good overall model accuracy. The MAPE values of Models BV and IV are similar. The similarities in statistical estimates, scatter plots, σ^2 , and MAPE of Models BV and IV indicate that the corrosion characteristics and capacities of strands exposed to BV and IV are similar.

Model OV

As in the BV and IV, OV samples exhibit almost similar sensitivity toward all the regressors used in the model. High confidence levels on parameter estimates are evident from their reasonably small SDs. The reasonably good prediction accuracy is exhibited by the scatter plot in Fig. 6(d), with most data points within the $\pm\sigma$ band. The MAPE is 2.8% (similar to the MAPE of Models BV and IV). These results indicate that the effect of BV, IV, and OV conditions on SC and capacity reduction is very similar or identical for practical purposes. In other words, a strand in a PT column with a vertical profile or a strand in a PT girder with

inclined profile may experience similar reduction in capacities, provided the moisture and chloride conditions are identical.

Model PV

Model PV indicates that the capacity of strands, when exposed to PV conditions, is more sensitive to t_{WD} than to $\%Cl^-$ and $\%Cl^- \times t_{WD}$. Model PV exhibits good confidence in mean estimates of θ_1 , θ_2 , θ_3 , and θ_4 because of their small SDs. These estimates and small model variance show that Model PV can confidently predict capacities in close agreement with the observed values. As evident in Fig. 4, for PV samples, the variability in the data are very small for 12-month samples [shown with rhombus data markers in Fig. 6(e)]. Fig. 6(e) also shows that most data fall within the $\pm\sigma$ band. The lower variability among the 12-month samples also resulted in a reduced scatter of the PV samples when compared with those of BV, IV, and OV samples. Due to the same reason, Model PV exhibited a smaller MAPE (1.6%) and variance than Models BV, IV, and OV. In summary, Model PV can provide good predictions of capacity of strands that are exposed to PV conditions that may be found in PT ducts with a horizontal profile.

As noted before, it may be difficult to determine the actual number or distribution of each type of voids present in a PT

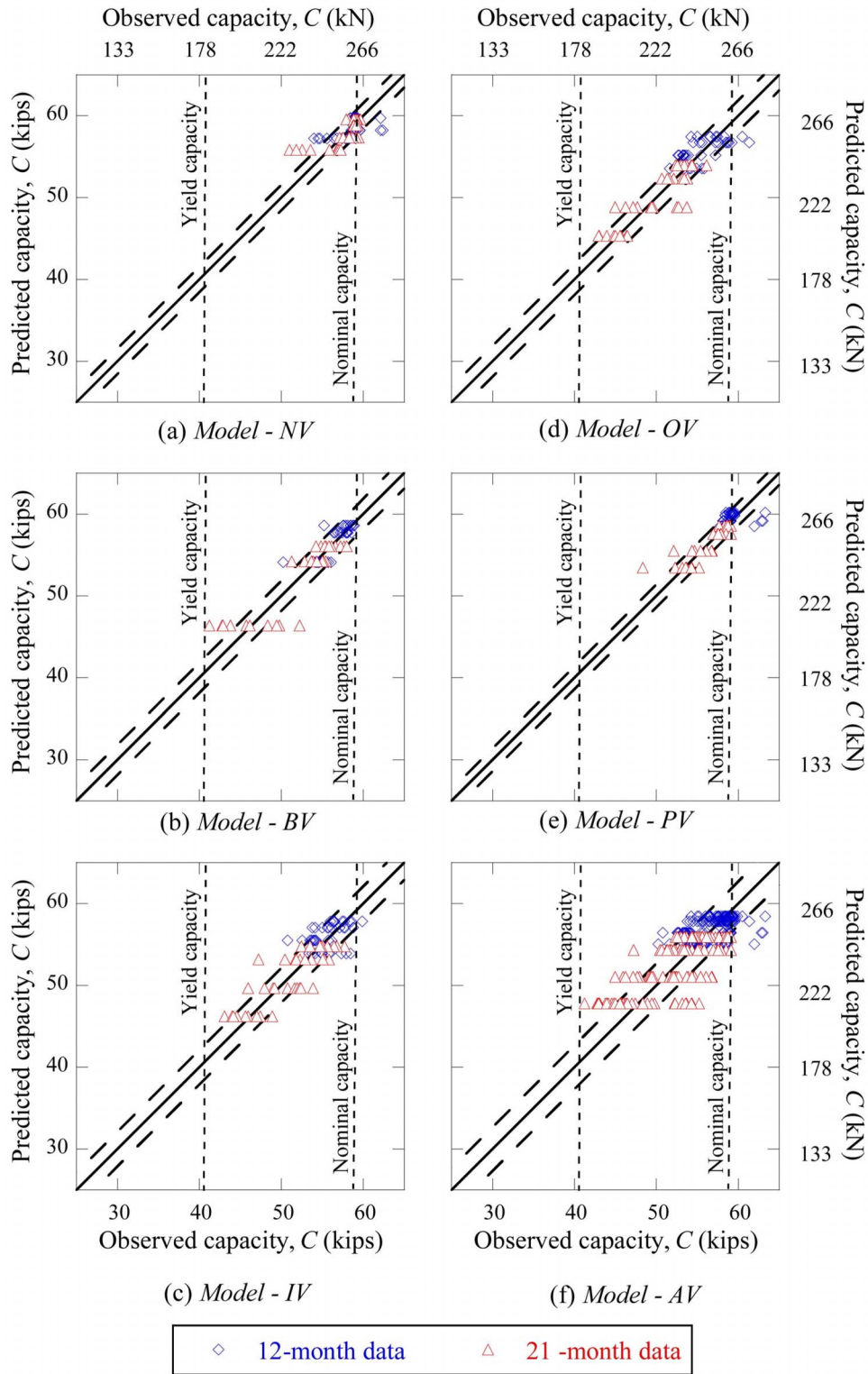


Fig. 6. Comparison between observed and predicted capacities from all six probabilistic models

system. In such cases, Model AV, which considers a uniform and equal distribution of different VT (except NV), may be appropriate or practical.

Model AV

Model AV was developed using all 304 data points from the pristine BV, IV, OV, and PV samples. The parameter estimates indi-

cate that the capacity is more sensitive to t_{WD} than to $\%Cl^-$ and $\%Cl^- \times t_{WD}$. The posterior means for this model have reasonably small SDs indicating good confidence in the mean estimates. Also, the reasonably small σ^2 and MAPE (i.e., 4.0%) and the fact that only a small percentage of data falls outside the $\pm\sigma$ band [Fig. 6(f)] indicate a reasonably good model accuracy. Although Model AV exhibits the largest MAPE among all six models, it is

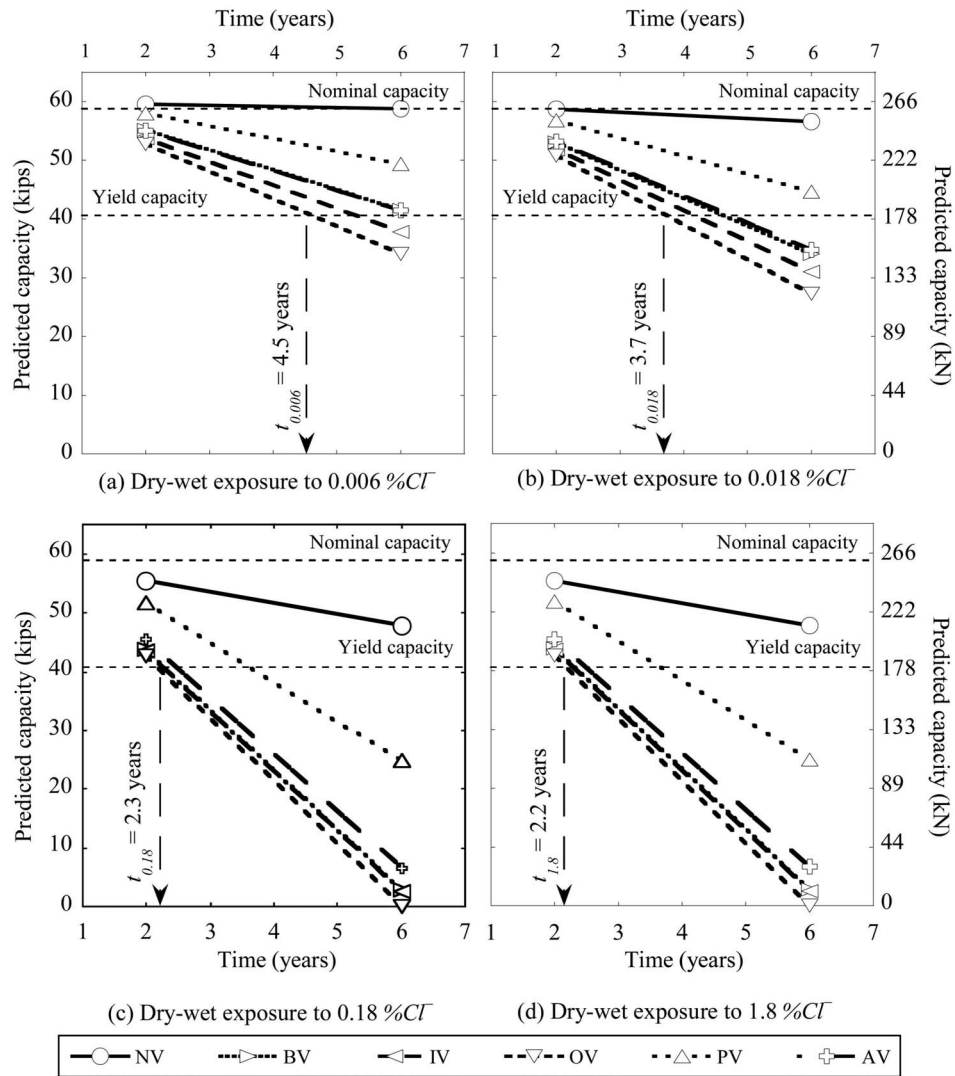


Fig. 7. Extrapolated strand capacities for different conditions using all six probabilistic models

a reasonably good value for practical structural assessment of PT bridges. In summary, Model AV can be used for general assessment of strand capacity in PT bridges when voids are known to be present but their types or characteristics are unknown.

Practical Applications

According to ASTM A416/A416M-06 specifications, posttensioning strands are produced to meet the mechanical property standards only and its chemistry is not specified. However, Table 3 provides the chemical composition of the steel used in this study. The mean and SD of the tension capacity of the uncorroded strands used in this study were found to be 59.27 (263.7 kN) and 0.29 kips (1.3 kN), respectively, indicating a very small CoV (i.e., 0.0049). This mean value meets the MUTS as required by the standard. The elastic modulus of the strand was 2.8×10^4 ksi (1.93×10^5 N/mm²) and is similar to expected values. The strands used in this study were procured from a major strand manufacturer in the United States and meet all specified requirements. As such, it is assumed that the strands used in this study represent the strands used in practice. Therefore, the probabilistic models developed in this document should be applicable to the strands in practice.

Table 3. Chemical Composition of ASTM-A416 Strands

Element	Sample 1	Sample 2
Al	0.0003	<0.01
C	0.841	0.842
Cr	0.029	0.032
Cu	0.120	0.115
Mg	0.018	0.007
Mn	0.811	0.819
Mo	0.0007	0.0008
N2	0.0436	0.0079
Nb	0.039	0.022
Ni	0.050	0.071
P	<0.01	0.0001
S	0.010	0.010
Si	0.241	0.230
Sn	<0.01	<0.01
Ti	0.001	0.003
V	0.081	0.082
Fe	Remaining	Remaining

The six probabilistic models developed in this paper can be used for predicting the remaining strand capacity when various void, moisture, and chloride conditions exist in PT bridges. It shows that when voids exist, the predicted capacities of strands dropped below the nominal capacity within approximately 2 years. However, the capacity remained higher than yield capacity for up to approximately 4.5, 3.7, 2.3, and 2.2 years, respectively, for the WD conditions with 0.006, 0.018, 0.18, and 1.8%Cl⁻, respectively. Note that these laboratory WD conditions are typically more severe than the field WD conditions. These times are shown by the vertical dashed arrows in Fig. 7. This shows, especially for conditions where WD cycles can be numerous, that the frequency of inspection and structural assessment of PT bridges should be performed on a regular basis. The inspection frequency should depend on the likelihood of water and/or chloride infiltration into the ducts. Frequent walk-through inspections could detect infiltration of moisture and chlorides into PT ducts. Repairs that prevent this ingress could mitigate further corrosion-induced strand failures, especially on those bridges with high importance factors. However, the moisture should be removed from the ducts before the repair work.

The authors recognize that the models have some limitations on their predictive capability for field conditions. However, this paper should be considered as a step toward the development of field models with better predictive capability for field conditions. Research is underway on correlating the findings in this article with actual bridge performance. The number and durations of WD cycles in the SC test program can be compared with the number and durations of WD cycles in the PT bridges and then the relationship between laboratory and field performances can be determined.

Conclusions

Based on the results from a 12- and 21-month SC test program (with 384 specimens), six probabilistic models were developed to estimate the capacity of 0.6-in. (15 mm) diameter low-relaxation seven-wire strands in PT bridges that have voided tendons with direct exposure to moisture and/or chlorides. The MAPE of the probabilistic capacity models were $\leq 4\%$ indicating a reasonably good overall model accuracy. The strands inside fully grouted tendons (i.e., without voids) exhibited the lowest amount of corrosion and capacity reduction. The strands in grouted tendons with horizontal voids exhibited slightly higher capacity reductions than those in fully grouted tendons. In general, the strands in the OV, BV, and IV conditions experienced higher capacity reductions than those in the NV and PV conditions. To minimize SC and resulting failures of PT bridges with high importance measures, the frequency of inspection, structural assessment, and repair (if needed) should be performed at regular intervals depending on the exposure and structural conditions.

One of the limitations of the six probabilistic models presented is that they are useful only when void, moisture, and chloride conditions exist. Fortunately, most PT bridges in the United States are not exposed to such severe corrosive conditions. Research is underway at Texas A&M University to develop a correlation between the actual bridge conditions and laboratory conditions tested. Also, research is underway in developing probabilistic capacity models for stressed strands.

Acknowledgments

This research was performed at the Texas Transportation Institute and Zachry Department of Civil Engineering, Texas A&M University, College Station, Texas, through a sponsored project from the Texas Department of Transportation (TxDOT), Austin, Tex. This support is much appreciated. Continuous support from Keith Ramsey (program coordinator), Maxine Jacoby (project director), Brian Merrill, Dean Van Landuyt, Kenneth Ozuna, Steve Strmiska, Tom Rummel, and other TxDOT engineers are acknowledged.

References

- Akgul, F., and Frangopol, D. M. (2004). "Lifetime performance analysis of existing prestressed concrete bridge superstructures." *J. Struct. Eng.*, 130(12), 1889–1903.
- American Concrete Institute (ACI). (2003). "Protection of metals in concrete against corrosion." *ACI 222R-03*, Farmington Hills, Mich.
- American Segmental Bridge Institute (ASBI). (2000). *Interim statement on grouting practices*, American Segmental Bridge Institute, Phoenix.
- ASTM. (2006). "Standard specification for steel strand, uncoated seven wire for prestressed concrete." *A416/A416M-06*, West Conshohocken, Pa.
- Box, G. E. P., and Tiao, G. C. (1992). *Bayesian inference in statistical analysis*, Addison-Wesley, Reading, Mass., 113–122.
- Florida DOT (FDOT). (2001a). "Mid-bay bridge post-tensioning evaluation." *Final Rep. Prepared for Florida Dept. of Transportation*, Corven Engineering, Inc., Tallahassee, Fla.
- Florida DOT (FDOT). (2001b). "Sunshine Skyway Bridge posttensioned tendons investigation." *Rep. Prepared for Florida Dept. of Transportation*, Parsons Brinckerhoff Quade and Douglas, Inc., Tallahassee, Fla.
- Gardoni, P. G., Der Kiureghian, A., and Mosalam, K. M. (2002). "Probabilistic capacity models and fragility estimates for reinforced concrete columns based on experimental observations." *J. Eng. Mech.*, 128(10), 1024–1038.
- Melchers, R. E. (2003). "Modeling of marine immersion corrosion for mild and low-alloy steels. Part 1: Phenomenological model." *Corrosion (Houston)*, 59(4), 319–334.
- National Cooperative Highway Research Program (NCHRP). (1998). *Durability of precast segmental bridges*, R. W. Poston, and J. P. Wouters, eds., *Transportation Research Record. 15*, Transportation Research Board, Washington, D.C.
- Pillai, R. G. (2009). "Electrochemical characterization and time-variant structural reliability assessments of post-tensioned, segmental concrete bridges." Ph.D. dissertation, Zachry Dept. of Civil Engineering, Texas A&M Univ., College Station, Texas.
- Poston, W. R., Frank, K. H., and West, J. S. (2003). "Enduring strength." *Civ. Eng. (N.Y.)*, 73(9), 58–63.
- Post-Tensioning Institute (PTI). (1998). *Acceptance standards for post-tensioning systems*, Phoenix.
- Post-Tensioning Institute (PTI). (2003). *Specification for grouting of post-tensioned structures*, Phoenix.
- Ryan, T. P. (2007). *Modern engineering statistics*, Wiley-Interscience, Hoboken, N.J.
- Schupack, M. (2004). "PT grout: Bleedwater voids." *Concr. Int.*, 26(8), 69–77.
- Trejo, D., Pillai, R. G., Hueste, M. D., Reinschmidt, K., and Gardoni, P. (2009a). "Parameters influencing corrosion and tension capacity of post-tensioning strands." *ACI Mater. J.*, 106(2), 144–153.
- Trejo, D., Hueste, M. D., Gardoni, P., Pillai, R. G., Reinschmidt, K.,

Kataria, S., Im, S., Gamble, M., and Hurlebaus, S. (2009b). "Effects of voids in grouted, posttensioned, concrete bridge construction." *Rep. No. 0-4588*, Texas Transportation Institute, Texas Dept. of Transportation, Austin, Tex., (<http://tti.tamu.edu/documents/0-4588-1-Vol1.pdf>).

Woodward, R. J., Cullington, D. W., and Lane, J. S. (2001). "Strategies for the management of posttensioned concrete bridges." *Current and future trends in bridge design, construction, and maintenance—2*, P. C. Das, D. M. Frangopol, and A. S. Nowak, eds., Thomas Telford, London, 23–32.